DOI:10.13878/j.cnki.jnuist.2018.03.007

W.N.D.S JAYARATHNA[1,2]　杜岩[1,2]　张玉红[1]　孙启伟[1,2]

基于卫星和 Argo 观测的阿拉伯海中北部海表盐度季节和年际变化

摘要

基于美国国家航天局(NASA)发射的水瓶座(Aquarius/SAC-D)卫星和欧洲航天局(ERA)发射的土壤湿度与海洋盐度(SMOS)卫星的观测资料,以及 Argo 海表盐度资料,重点分析了阿拉伯海中北部海表盐度的季节和年际变化.年平均情况下,Argo、Aquarius 和 SMOS 表现出相似的海表盐度分布形态,均表现了阿拉伯海中北部高达 36.5 psu 的高盐特征.阿拉伯海中北部海表盐度在 2—3 月出现最低值,在 4 月之后快速升高,并在夏季西南季风的成熟阶段达到最高.阿拉伯海中北部海表盐度显著的季节变化与季风风场引起的大量蒸发和平流输送相关.夏季风期间,Ras al Hadd 急流将来自阿曼湾的高盐水向东向南输送到阿拉伯海中北部海域,使海表盐度升高并达到最高值;冬季风期间,冬季风环流系统在印度半岛西侧海域形成向北的低盐水输送,造成阿拉伯海中北部海表盐度降低.该低盐水平流在冬季风后期能够影响到阿曼海.阿拉伯海中北部海表盐度年际变化主要与季风驱动的季风环流系统的变化相关,尤其是冬季风期间向北流动的印度西侧沿岸流的强弱与该区域海表盐度年际变化关系密切.

关键词

阿拉伯海;海表盐度;季风;平流;蒸发;季节和年际变化

中图分类号 P731

文献标志码 A

收稿日期 2018-04-19

资助项目 国家自然科学基金(41525019,41506019);国家海洋局项目(GASI-IPOVAI-02)

作者简介

杜岩(通信作者),男,博士,研究员,研究方向为海气相互作用.duyan@scsio.ac.cn

1 中国科学院南海海洋研究所 热带海洋环境国家重点实验室,广州,510301

2 中国科学院大学,北京,100049

0 导读

本文原文为英文,希望感兴趣的读者进一步关注原文.

北印度洋北部是地理上的热带海域,但北印度洋的两个海盆——阿拉伯海和孟加拉湾,周边的气候差异非常大.阿拉伯海受周边沙漠气候的影响,中北部海域常年蒸发大于降水,海表净损失淡水,表现出全球副热带海域的高盐特征;孟加拉湾受周边热带雨林气候的影响,有丰富的降水和地表径流淡水输入,海表净得淡水,是热带大洋中盐度最低的海域.北印度洋冬季出现逆时针流动的东北季风环流系统,夏季出现顺时针流动的西南季风环流系统,它们对维持北印度洋两个海盆的长期盐度平衡起着重要的作用.阿拉伯海中北部海域是北印度洋高盐水形成和向南输送的关键海域,研究该海域海表盐度的变化对了解该区域的海洋动力过程和气候变化有着重要的意义.

本文利用美国国家航天局(NASA)发射的水瓶座(Aquarius/SAC-D)卫星和欧洲航天局(ERA)发射的土壤湿度与海洋盐度(SMOS)卫星的观测资料,以及 Argo 海表盐度资料研究了阿拉伯海中北部海表盐度的季节和年际变化.结果表明:三种观测资料都能很好地表现阿拉伯海中北部的高盐分布特征,但是 SMOS 观测资料由于设计上的问题,受陆地影响的噪音无法去除,不能用于季节和年代际变化的研究.Argo 和 Aquarius 观测到的海表盐度变率相似,但 Argo 观测到的海表盐度较 Aquarius 的高.这是由于 Argo 浮标观测的海表盐度是大约 5 米深度上的,而 Aquarius 观测的是海表面上的盐度.

阿拉伯海中北部海表盐度最高值出现在北部并向南递减.受平流和淡水通量的影响,该海域的海表盐度表现出显著的季节变化特征.夏季风期间,Ras al Hadd 急流将来自阿曼湾的高盐水向东向南输送到阿拉伯海中北部海域,使海表盐度升高并达到最高值.阿拉伯海中北部的高盐水在夏季风末期被输送到阿拉伯海东南部海域.冬季风期间,冬季风环流系统在印度半岛西侧海域形成向北的低盐水输送,造成阿拉伯海中北部海表盐度降低.该低盐水平流在冬季风后期能够影响到阿曼海.阿拉伯海中北部海表盐度年际变化主要与季风驱动的季风环流系统的变化相关,尤其是冬季风期间向北流动的印度西侧沿岸流的强弱与该区域海表盐度年际变化关系密切.

Seasonal and interannual variability of sea surface salinity in the central north Arabian Sea based on satellite and Argo observations

W.N.D.S JAYARATHNA[1,2] DU Yan[1,2] ZHANG Yuhong[1] SUN Qiwei[1,2]

1 State Key Laboratory of Tropical Oceanography, South China Sea Institute of Oceanology, Chinese Academy of Sciences, Guangzhou 510301

2 University of Chinese Academy of Sciences, Beijing 100049

Abstract This study mainly focuses on the seasonal and interannual variability of sea surface salinity (SSS) in the Central North Arabian Sea (CNAS) by using Aquarius/Satelite de Aplicaciones Cientificas-D (SAC-D) and the Soil Moisture and Ocean Salinity (SMOS) satellite measurements, and gridded Argo field data from 2011 to 2015. The mean state of spatial SSS variation is consistent among Argo, Aquarius, and SMOS datasets. CNAS has relatively higher SSS with mean of 36.5 practical salinity unit (psu). The lowest SSS in the studied area occurs during February to March and rapidly increases after April. SSS reaches its maximum during the mature phase of southwest summer monsoon period. The CNAS SSS shows significant seasonality due to the advection and evaporation associated with high monsoon winds. As a result of southward advection, high salinity water from the Gulf of Oman and the existence of Ras al Hadd Jet, contribute to the highest SSS during the southwest monsoon period in the CNAS. Northwestward advection of low salinity water from the south, leads to the salinity reduction during northeast monsoon periods in the region. This low SSS advection can reach the Oman Sea during the late winter monsoon period. The interannual variability of the CNAS SSS is mainly associated with the monsoonal ocean circulation that triggered by the regional monsoon variation. In particular, it depends on the strength of the northeastern Arabian coastal currents, which transport low salinity water northwestward.

Key words Arabian Sea; sea surface salinity; monsoon; advection; evaporation; seasonal and interannual variation

1 Introduction

Salinity is considered as an important index for measuring the global climate system. North Indian Ocean (NIO) salinity is mainly regulated by precipitation, evaporation and the fresh water influx from the continental rivers. The NIO is divided into two semi-closed seas, the Bay of Bengal (BoB) and the Arabian Sea. Although they are in similar latitudes and influenced by similar atmospheric forcing, their hydrological cycles are distinctly different. The Arabian Sea loses its freshwater due to the excess evaporation (2 m/a) along with extreme surface heat loss, while the BoB is having high fresh water input with overloaded precipitation and river runoff[1]. The excess evaporation in northern Arabian Sea leads to high salinity dense water, which further have impacts on the large scale ocean circulation in the marginal sea[2]. An annual scale hydrological imbalance presents between the Arabian Sea and the Bay of Bengal. The inter-basin exchange due to the reversing monsoon winds helps to maintain the long term salinity balance in these two basins[3].

Northern Arabian Sea (NAS) is a critical ocean environment with much large impact on the climate variability. It is considered as a semi-enclosed sea, and surrounded with a coastal belt from north. The eastern boundary of the NAS is India and Pakistan, while the west is Oman and Somali coasts[4]. The sea surface salinity (SSS) of NAS changes between 35.4 and 36.7 psu, descending gradiently from north to south[5]. The high salinity water from Persian Gulf and Red Sea influences the water mass properties of the Arabian Sea.

Tropical monsoons play a significant role in SSS distribution, maintaining the salinity balance in the Arabian Sea. With the activation of southwesterly winds, upwelling begins in Somalian region. It becomes more prominent during the late phase of southwest (SW) monsoon. During March to April, northward advection of low salinity water from south is dominated in the

western NAS. Then the low salinity water begins to be replaced by high salinity water advection from north during the mature phase of SW monsoon (June-August)[6]. Summer monsoon current (SMC) in the southern Arabian Sea is set in motion to flow eastward during May. Throughout the mature phase of SW monsoon, Somali current and coastal current of Oman flow eastward and southeastward respectively across the Arabian Sea. Flowing around Lakshadweep low, they reach south of Sri Lanka by the end of August[6]. At the end of the SW monsoon, SMC and southward moving West Indian Coastal Currents (WICC), bring the Arabian Sea high salinity water into the BoB. As a result of that, SSS increases in the western BoB during late phase of SW monsoon[7]. In winter (December to February), downwelling occurs in Omani coast with favorable northeast monsoon winds. Winter monsoon current (WMC) and West Indian Coastal Current (WICC), get to flow westward and northwestward, respectively. This helps to advect low salinity water from the BoB to the southeastern Arabian Sea[8]. The northeasterly winds, coming from the Asiatic continent which is dry and cold, increase the SSS followed by excess evaporation in NAS[9].

At early stage, the in situ salinity and temperature sampling were limited to the shipping lines called "ships of opportunity"[10]. With understanding of the value of the ocean salinity, researchers have developed new technological methods to measure in situ salinity and temperature. Conductivity, temperature, and depth (CTD) techniques, ocean gliders, surface drifters and space platforms, such as satellites, are equipped to measure SSS in global oceans. Argo program of profile float is one of the most important in-situ data measuring method, deploying all over the ocean in nowadays[11]. Higher spatial and temporal resolutions can be achieved by satellite observations. Soil Moisture and Ocean Salinity (SMOS) mission launched by the European Space Agency and the "Aquarius" mission launched by National Atmospheric and Space Administration and the Space Agency of Argentina provide reliable and long term observation of sea surface salinity[12].

As the salinity maintains the water mass properties in the ocean, several studies have been done over the water mass properties in the Arabian Sea. They have studied about the formation and spreading of the Arabian Sea high salinity water masses in the northern Arabian Sea and its importance to the region[2,4,13-14]. The high salinity water of marginal seas in the Arabian Sea and its seasonal changes in the upper ocean were investigated during the SW monsoon seasons. In recent studies, scientists mainly focused their interest on the climate variability and associated climate modes[15-16]. They found that the inter-annual SSS variability makes good responses to the near equatorial region which is associated with Indian Ocean Dipole. Studies about the salinity budget indicates that, anomalies near the equator were due to the prevailing zonal advection[15,17]. The seasonal variability of sea surface salinity has most pronounced signature in the coastal regions of the northern Bay of Bengal, northwestern Arabian Sea, as well as in the southeastern Arabian Sea[2,7-8]. Recent high resolution SSS observations from satellites are also used to study the SSS in the Indian Ocean, from seasonal to interannual time scales[16,18-20].

Most of the studies about SSS variations in North Indian Ocean have been carried out near the eastern, western and equatorial boundaries. Due to the lack of SSS observation data in the NAS, there are difficulties to understand the extent of seasonal changes in the region and their associated dynamics. We select the study region of Central North Arabian Sea (CNAS) (62 – 67° E, 18–24°N) and use the Aquarius, SMOS satellites and Argo SSS measurements to evaluate the regional SSS variations on seasonal and inter-annual time scales.

The arrangement of the paper is summarized as follows. Section 2 gives data description and methodology. Section 3 is result and discussion, including comparison of different kinds of data, statistical validation for satellite and Argo salinity, description of the mean state of the SSS, and seasonal and interannual variation of SSS in the CNAS. At the end the summary and conclusions are given in section 4.

2 Data and method

Argo gridded monthly products are used as in situ

measurements.These Argo floats give a regular data coverage in the open ocean.The deploying range is from subsurface (1-5 m) to 2 000 m into the deep with an average spatial resolution of 300 km.In addition,World Ocean Atlas 2009 (WOA 09) was used as the climatological monthly temperature and salinity products to do comprehensive studies.Argo monthly composite temperature and salinity data can be found in Scripps Institution of Oceanography,and here the data will be considered from January 2004 to December 2015.

On June 10, 2011, Aquarius satellite/SAC-D satellite mission was launched for long term observations of SSS in world oceans.It has a sun-synchronous polar orbit at 657 km above earth and repeats itself once a week.Aquarius is equipped with one scatterometer and three radiometers to collect SST.Salinity is derived by using these collected SST values in other flat forms.Surface roughness taken from scatterometer is used to correct this data.Aquarius monthly composite, level-3 standard version (3.0) data with 1°×1° resolution,are available for public users in Ocean Data Processing System (ODPS) of NASA Goddard Space Flight Center (GSFC)[21].For this research the studied duration for Aquarius is January 2012 to December 2014.

SMOS mission was started on November 2,2009, as a joint plan of ESA/French Space Agency Earth observation Program.The main purpose of this satellite is to measure land soil moisture and ocean salinity.It uses an aperture synthesis radiometer to measure the brightness temperature emitting from earth surface.It has altitude of 758 km and repeats in every 3 days.These data are available as monthly composite of ESA level-3 SSS in quarter degree resolution.SMOS data from January 2011 to December 2015[21](available at Centre Aval de Traitement des Données SMOS website) are used in this comparative study.

Precipitation data is from Global Precipitation Climatology Project (GPCP)[22] from 2000 to 2015,evaporation data is from Objective Analyzed air-sea Fluxes (OAFlux)[23] from 2000 to 2016,surface wind forcing data is from Advanced Scatteromete (ASCAT)[24] from 2008 to 2017,and monthly satellite field derived ocean surface currents data is from Ocean Surface Current Analysis Real-time (OSCAR) of the National Oceanic and Atmospheric Administration (NOAA)[25] from 2000 to 2016.

SSS anomalies for satellite datasets were calculated by subtracting the climatological monthly mean of Argo SSS for 2004-2015.Anomalies for the other parameters were calculated by removing their own climatologies for the specific time periods.

3 Results and discussion

3.1 SSS in the northern Arabian Sea

Mean state of Northern Arabian Sea (NAS) surface salinity is obtained from comparative study between satellite and Argo observation data.Argo SSS data is averaged from January 2004 to December 2015, Aquarius SSS data is averaged from January 2012 to December 2014,and SMOS SSS data is averaged from January 2011 to December 2015.The three data sets show a similar SSS variation in the NAS region (Fig.1).Both satellite derived SSS maps have considerable detailed spatial structure for the mean state of SSS compared with the Argo. All of the salinity data sets display a clear result of higher salinity in the northern Arabian Sea region with the descending gradient towards the south.

The annual mean SSS in the studied area of Central North Arabian Sea (CNAS) (62-67°E,18-24°N) (shown in Fig.1a as a rectangle) is 36.5 psu. Northeast (NE) winter monsoon period can be considered as December to the following February,and SW summer monsoon from June to August.The contrast in ocean dynamics during the two main monsoon periods can be clearly identified in Figure 1. The dominant northeastward moving surface current and surface winds in the region maintain very distinct patterns of SSS in the NAS during summer.The higher SSS values in the north of 15°N are resulted from the strong advection from north.In contrast,low SSS values are observed toward the equator due to the low salinity water advection from the eastern Indian Ocean as well as the excess precipitation in the region[26].Northern part of the Arabian Sea shows low mean SST value compared with the equatorial region (north of 12°N),where heat loses due to

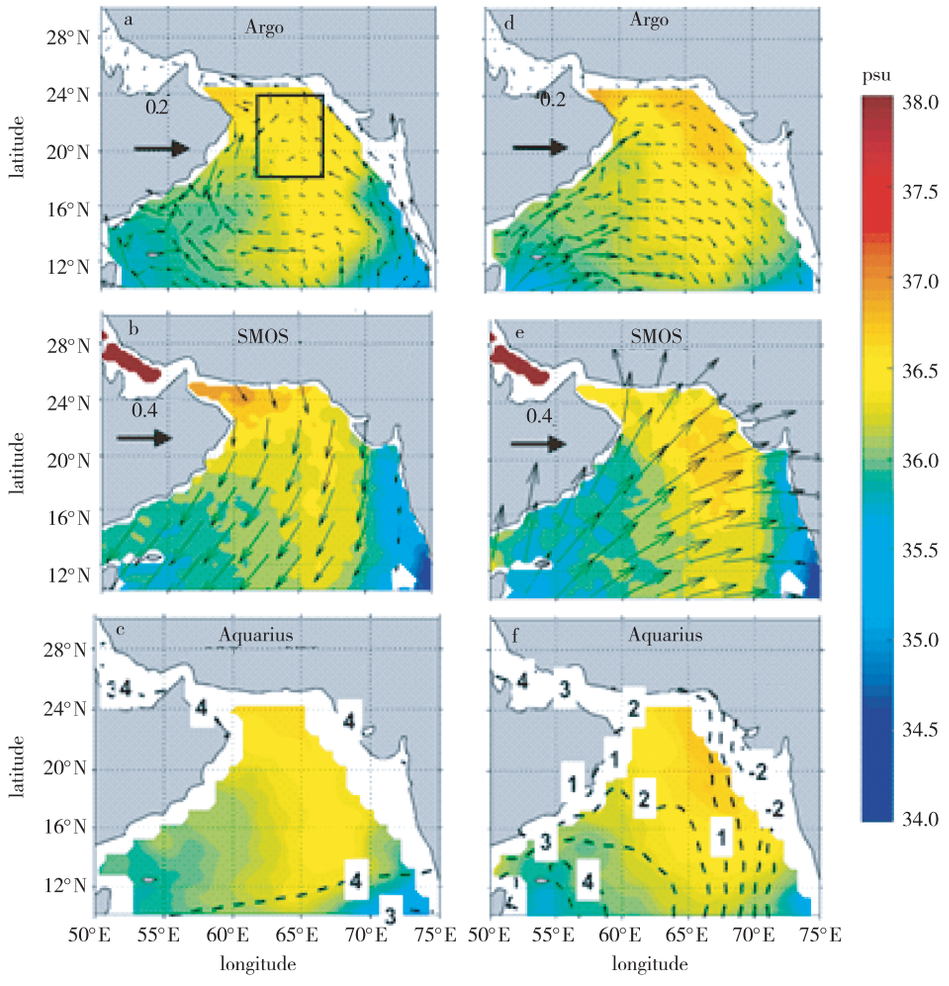

Fig. 1 Seasonal distribution of SSS from three different data sources (shaded, unit: psu) as Argo, SMOS, and Aquarius, superimposed with seasonal means of OSCAR ocean surface currents, ASCAT surface wind, E-P, and OISST sea surface temperature: (a)-(c) winter (December-February) and (d)-(e) summer (June-August); (a) and (d) Argo salinity superimposed in OSCAR surface currents (vectors, unit: m/s), (b) and (e) SMOS superimposed in ASCAT surface (vectors, unit: m/s), (c) and (f) Aquarius salinity superimposed in E-P ((OAFlux and GPCP) (contours, unit: mm/day); the study region is the Northern Central Arabian Sea (NCAS) (62-67°E, 18-24°N), as shown in (a) as a rectangle

the surface cooling[3].

3.2 Features of Argo and satellite SSS

For these data sets, various error metrics are computed. Mean SSS from Aquarius and SMOS satellite show underestimation than that of Argo (Table 1) in the NAS region. Argo shows 0.03 psu higher in the CNAS than the satellites measurements. Argo and Aquarius show strong positive correlation than the SMOS (Fig.2a). Monthly analysis of Aquarius satellite data shows significant agreement with in-situ Argo data[18]. Although the standard deviations are similar for the 3 data sets, Argo shows a low SSS towards the central equatorial Arabian Sea region (62-67°E, 5°S-5°N) (figure not shown) which is similar to the previous results of low SSS values for Argo measurements under the intensive rainfall in equatorial region[27]. There is considerable discrepancies between SMOS and Argo SSS according to spatial components, as the SMOS satellite values fall off from land induced contaminations near the continents. And therefore SMOS SSS values are considerably inconsistent with that of Argo[28]. The mean state difference between Argo and Aquarius is shown in Figure 2b. Positive difference presents near the coastal regions (north, and northeast), and negative difference exists at the middle of the region. As the Argo

Table 1 Statistical comparison of monthly Aquarius (2012-2014), SMOS (2011-2015) satellites and Argo (2011-2015) SSS observations

Region	Mean SSS/(psu)			Standard deviation/(psu)		
	SMOS	Argo	Aquarius	SMOS	Argo	Aquarius
NAS (18-24°N;62-67°E)	36.482 1	36.525 9	36.495 6	0.412 4	0.184 3	0.171 4
CEqAS (5S-5°N;62-67°E)	35.265 8	35.251 6	35.278 6	0.284	0.288 5	0.276 8

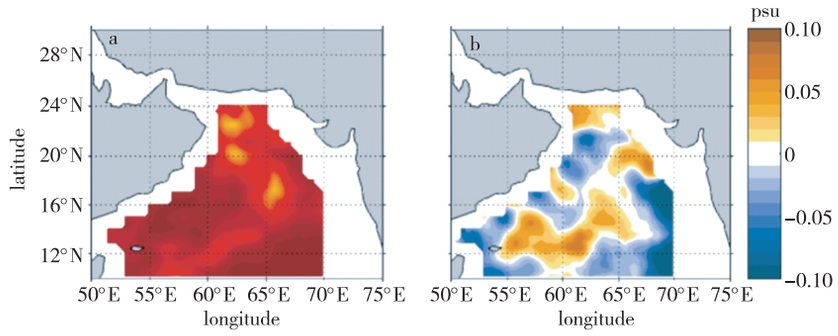

Fig. 2 (a) Correlation coefficient between Aquarius SSS and Argo SSS, with shading indicates regions significant at 0.05 level for Argo; (b) Mean SSS difference (shading, unit: psu) between Argo and Aquarius from January 2011 to December 2014

are mostly deployed in deep waters, and not having enough sampling data, the values between Argo and Satellites can be varied[18,27,29]. Thus dissimilarities occur in data values when doing the Argo objective interpolation in the insufficient sampling locations[29].

Paired assessment between SSS datasets is done over the selected region indicated by box in Figure 1. Argo and Aquarius datasets are more consistent with each other than with that of SMOS dataset, by showing higher *R*-square values (Fig. 3a). Although the SMOS captured the mean well, it has fabricated RMS value for the NAS which will be discussed in next sections. As a result of that, we will only consider the Argo and Aquarius satellite measurements hereafter for the seasonal and interannual SSS evaluations.

3.3 Seasonal variation of SSS

The salinity in the Northern Arabian Sea has intense seasonal variability, which is associated with monsoon cycle. The SSS, winds, surface currents, evaporation, and precipitation show enormous discrepancies coupled with space and time (Fig.4). SSS variations for the latitude-time diagrams are more similar for the Argo and Aquarius. Zonally averaged SSS and the other physical parameters in the selected region have interseasonal variation which are shown in Figure 4 a-b. The salinity reaches the maximum in north of 22° N and its meridional salinity descending gradient towards the equator is sustained throughout the year. The south of 22° N shows the strongest seasonal variations for SSS, including all other parameters.

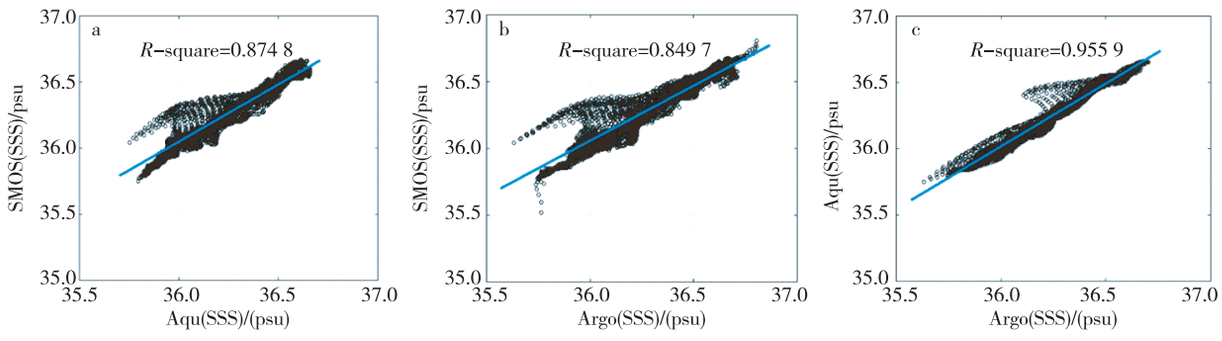

Fig. 3 Scatter diagrams of SSS between satellites and Argo in Northern Arabian Sea, (a) SMOS and Aquarius, (b) SMOS and Argo, and (c) Aquarius and Argo

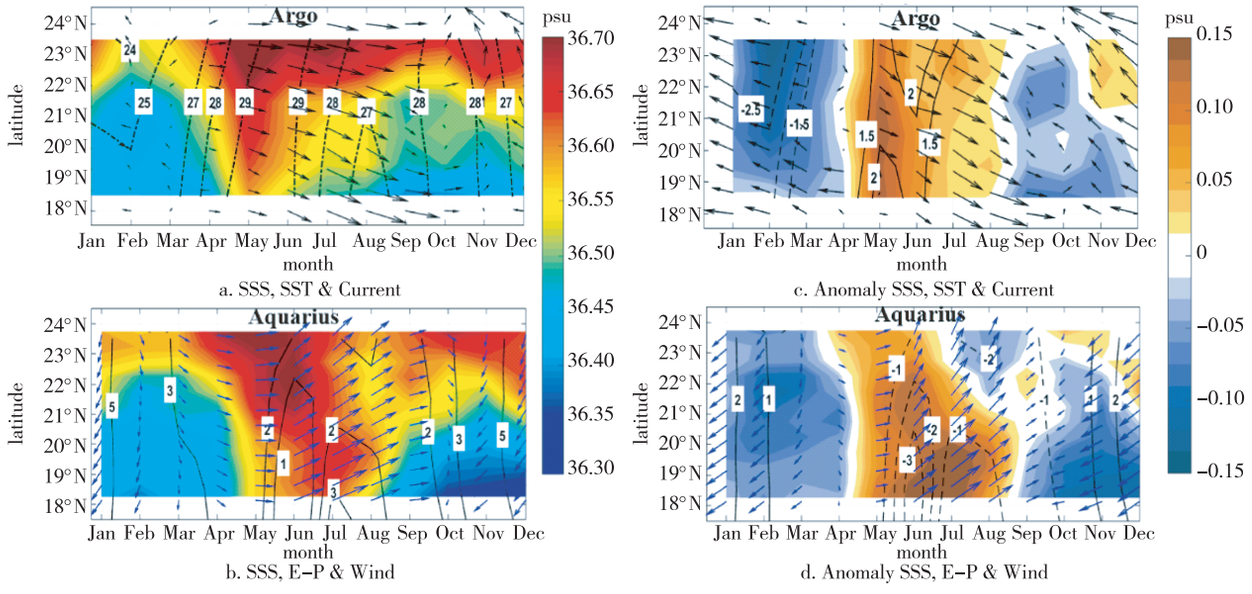

Fig. 4 Latitude-time diagrams of the selected area (longitude 62-68°E): (a) Aquarius SSS (shaded, unit: psu), NOAA SST (contour, unit: ℃), and OSCAR currents (vector, unit: m/s); (b) Aquarius SSS (shaded, unit: psu), E-P (contour, unit: mm/d), and ASCAT wind (vector, unit: m/s); (c)-(d) seasonal anomalies of (a) and (b) respectively (multi-year climatology removed from each parameter)

Result from the Argo and Aquarius satellite SSS shows higher SSS during SW monsoon period. The increases of the SSS and SST in CNAS begin from the end of April and the maximum values for both can be observed during the May-June period when the early phases of SW monsoon respectively appear. During this period, the maximum salinity and the corresponding temperature are 36.7 psu and 29 ℃ (Fig. 4a). The south westerly winds are directed to northeastward (Fig. 4b). Previous studies show that the SSS decreases during the SW summer due to the low SSS water advect from the OMAN and Somalian upwelling to the CNAS region[5,13]. But in point of fact, this reduction appears during the end of the SW monsoon (September) near south of 19°N (Fig. 4a) because of the lag time response of salinity compared to the currents. During May to September, the winds during SW monsoon are constantly directed to the northeastward (Fig. 4b), which triggers strong northward western coastal currents and strong southeastward currents in the open ocean (Fig. 4a). This southward components advect high salinity water into the study region from the most north western parts of the Arabian Sea where highest SSS water persists. These SSS increases during the SW monsoon period are probably due to the warm high salinity water activation associated with East Arabian Sea's (EAS) western boundary current called Ras al Hadd jet (RAH)[30-31]. This current exists from May to September, and becomes energetic with SW monsoon wind establishment. It brings high salinity warm water from the Gulf of Oman and elevates surface temperature during SW monsoon period in the NAS (Fig. 4a). The results can be confirmed by the studies done by Lee in 2000[32]. The velocity and the strength of the RAH is highest during the transition period from NE monsoon to SW monsoon[30]. Highest value for the surface velocity near RAH, is dominating during the same time where the SSS exactly begins to increase in the study region (end of May) (Fig. 4a). The E-P couldn't explain the salinity increase during the May to June period. Although both SST and the SSS show their maximum values during particular time, E-P gets low positive values (Fig. 3b) during the period. It means that the evaporation would not be a driving factor for the SSS rising during early summer in the CNAS region. During September and October a reduction shows in SSS, which is caused by the low salinity advection by the western coastal current from south east Arabian Sea.

In the NE monsoon (December to February), dry and cold northeasterly winds cool the surface of the north eastern Arabian Sea. As a result of that, the surface salinity increases to more than 36.5 psu and SST drops to 24 ℃[1]. Anomalies of SSS in the north of 21°N show an increase in both Argo and Aquarius salinity measurements during winter, but not strong as that in summer (Figs.4c-d). The continued decrease of SSS in south of 20°N can be observed with the beginning of NE monsoon. Minimum values for the SSS appear during the end of February. Although the northeasterly winds are strong during the winter monsoon period, a western coastal current moves to northwestward along the western Indian coast, which has an opposite direction to the wind. Surface currents and winds during NE monsoon are not stronger than those during SW monsoon period[9]. These results suggest that the low salinity water in the south of CNAS during November to February is advected from the eastern Arabian Sea, which are formed in the Southeast Arabian Sea as well as in the equatorial region. The reduction of SSS in the region is associated with low salinity water advection from the south eastern part of the Arabian Sea via the eastern coastal currents of India called west Indian coast current (WICC) during Northeast (NE) monsoon period[33].

Argo and Aquarius satellite show similar SSS variations throughout the year for the studied region. As a result of that, Aquarius satellite and Argo can be used to study the regional salinity variation with an acceptable manner in CNAS. According to the seasonal anomalies, there are two negative phase of SSS and one strong and one small positive SSS anomalies in the CNAS during a year (Figs. 4c-d). The positive SSS anomalies appear to be in middle of the April for both Aquarius and Argo. But during some particular time, surface current and wind anomalies are relatively weak. Then the positive anomalies become stronger in June-July period. This positive anomalies appear in the entire region (18-24°N), and last until the end of August. Wind, currents and the SST show positive anomalies during the above mentioned time period (April to August). This positive SSS anomalies can be considered as the corresponding summer salinity increases in the region. But E-P displays a negative anomaly value during the period. To explain these negative E-P anomalies we need to do studies about the subsurface changes too. The positive SSS anomalies results for both satellite and Argo during the May to August period is consistent with findings of previous studies. The advection of dense water and the Ekman pumping from the north to the central basin during SW monsoon can initiate these positive SSS anomalies[34].

The second positive SSS anomalies appear in the north of 20°N during November for the Argo (Fig.4c), but in Aquarius it has already appeared at the beginning of October (Fig. 4d). Strong southwestward winds anomalies that appear during this period, suggest the activation of dry and cold northeasterly winds in winter, when they induce the excess evaporation and raise the surface salinity in the region[35]. In the meantime, negative SSS anomalies at south of 20°N, appear in November and become strong and persist as negatively during the end of NE monsoon in February. The strong northwestward current anomalies as well as the weak southwestward wind anomalies in the region provide evidence for the advection of low SSS water from the equatorial region and the west coast of India[1,31,34,36].

For the winter monsoonal anomaly study, February is considered as the mature phase of winter (Figs. 5a-b). Aquarius and Argo show similar SSS variation for the winter. In Figure 5a, it's clearly showed that negative anomalies extend up to the Sea of Oman in the mature phase of the winter monsoon in NAS. This negative anomalies appear due to the advection of low salinity water probably with WICC and other coastal currents in the north eastern Arabian Sea, indicated as northwestward moving surface current anomalies in Figure 5a[30]. Due to the dry and cold NE monsoon winds, while negative SST anomalies develop in the NAS, relatively positive anomaly values for E-P can be observed near the coastal waters of north western India (Figs.5a,b). And during this period positive SSS anomalies remain only at the southwestern part of the NAS, as the southward moving coastal currents of Oman shift

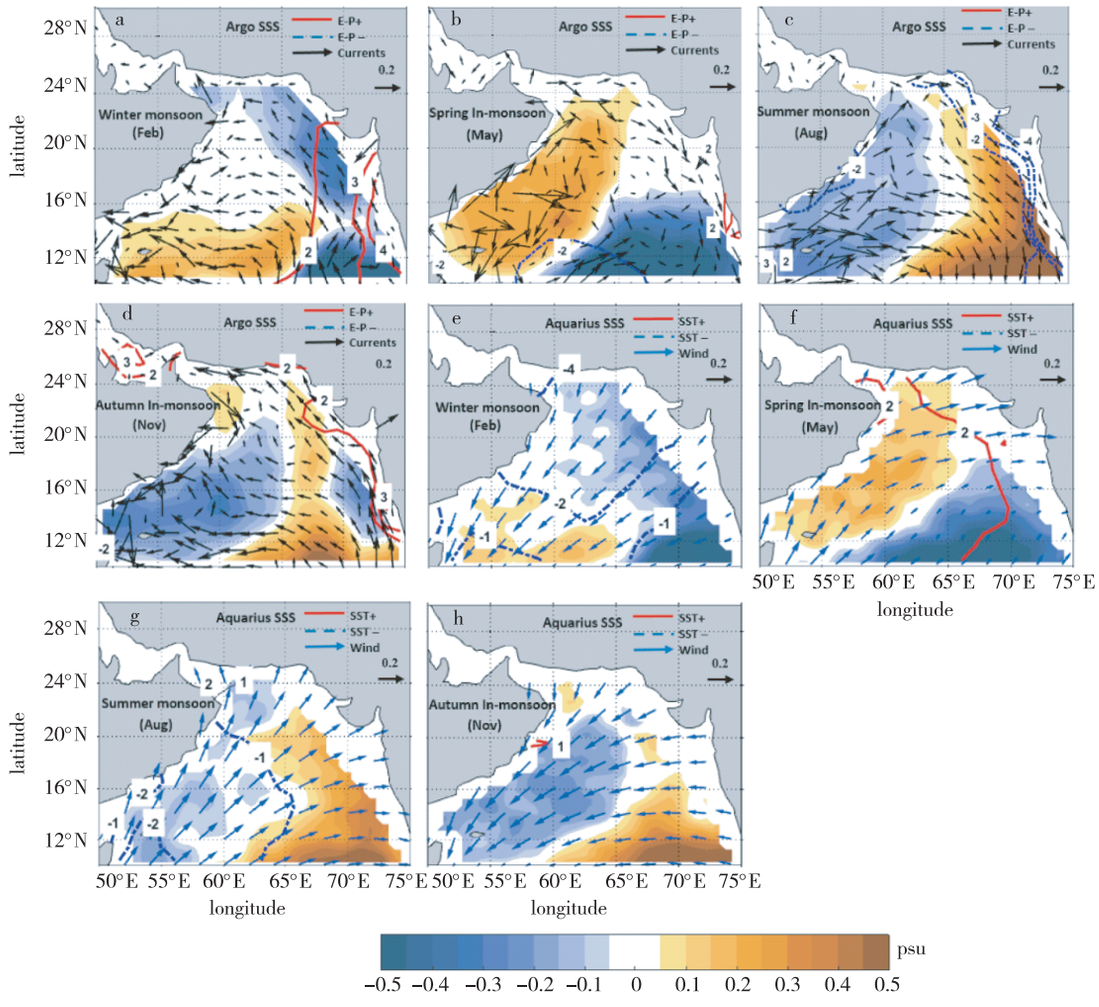

Fig. 5 Monthly averaged SSS anomalies (shaded, unit: psu) at different monsoonal seasons, where (a–d) for Argo SSS anomalies, surface current anomalies (black arrows, unit: m/s), and E-P anomalies (contour, red (+), dashed blue (−), unit: mm/day), and (e–h) for Aquarius SSS anomalies, surface winds anomalies (blue arrows, unit: m/s), SST anomalies (contour, red (+), dashed blue (−), unit: ℃)

the high salinity water more downward during winter. Transition period between the tropical monsoons are more related with annual variation of SST in the north Indian Ocean. In this study, the first inter-monsoon (spring inter monsoon) is considered as May, and November as the second inter-monsoon. Aquarius and Argo could display a similar pattern of interseasonal SSS anomaly variations in this study (Figs.5b, d, f, h).

During the first inter-monsoon, as a result of southwestward advected high salinity NAS waters in Omani coast, and northwestward advected low salinity south eastern Arabian Sea water in western Indian coast, positive SSS anomalies and negative SSS anomalies showed respectively in these two regions (Fig.5b). Positive SST anomalies during the first inter monsoon (Fig. 5f) appear due to the excess heating via strong incoming radiations. Although the wind anomalies during February are headed to southwestward direction in NAS, during May they have changed their direction as northeastward in the NAS, and clockwise changes can be observed toward the south.

NE moving surface currents and winds start to appear during May and become strong in August of SW monsoon period (Figs.5c, g). As the intertropical convergence zone (ITCZ) moves northward[37], higher precipitation probably causes the negative SST anomalies in the southwestern Arabian Sea (Fig.5g) during peaks of the SW monsoon. A negative SSS anomaly begins to

appear near the Oman and NA coastal regions where the coastal upwelling is strengthening. And the positive SSS anomalies are more prominent in the eastern Arabian Sea, due to advection of the high SSS water towards the east and central Arabian Sea associated with southeast moving surface currents (Fig.5c).

In the second inter monsoon (autumn inter monsoon), considered as November, distribution of SSS anomalies are almost opposite to the first inter monsoon (May) (Figs.5d,h). At this moment the advected low salinity water from south during SW monsoon period has been distributed to west and the center of the NAS[38], where it's indicated as negative SSS anomalies in the west. And the negative SSS anomalies near the western Indian coast in Figure 5d confirm the upwelled low salinity water during previous SW monsoon in this region. These negative SSS anomalies only appear in the Argo SSS measurements. The most probable reason is that, Argo indicates the 5 m below salinity measurements. Due to the southeastward advection of high salinity water from the NAS[39] during the SW monsoon, the salinity shows positive anomalies along the southeast coast of India during the second inter-monsoon period[2]. It reveals that the Arabian Sea high salinity water advects to the southeastern Arabian Sea, almost to the equatorial region.

3.4 Inter-annual variability

In this study, interannual variation of SSS is also considered for particular time periods relevant to the data source. Argo has been considered from 2004 to 2017, and Aquarius for 2012 to 2014. Interannual variation of RMS for both Aquarius and Argo shows large SSS variation near NAS above 18° N (Figs. 6a, b), where it's spreading toward south. This indicates that the studied region has more related interannual variability during the SW monsoon period. Aquarius shows stronger SSS variance than Argo, in particular area as it is only considered for 2 years' time. And differences in spatial RMS changes can be observed between Argo and Aquarius near eastern Arabian Sea, and the south central of 16°N (Figs.6a,b). It may be due to the less amount of sampling locations and the dissimilarity with corresponding point data distribution for the two data sets and as well as the unbalanced time-space data distribution, such as near the continents[40]. The land induced contaminations in SMOS measurements may cause the incorrect SSS results for interannual variability near the coastal region[27].

Time series of Aquarius and Argo show an extensive inter-annual variation for the CNAS (Fig.7a). Negative (positive) SSS anomalies were considered relevant to its lower (higher) position in the Argo climatological seasonal cycle. Both Aquarius and Argo observe similar inter annual variation from January 2012 to December 2014. Both show strong negative SSS anomalies during 2012. Since 2004, Argo reveals largest positive SSS anomalies between end of 2015 and 2016. The winter time SSS anomaly variation are compared with the northeast *V* component of the surface current (Fig. 7b). After 2008, it clearly shows that whenever there is a negative *V* anomaly, SSS will get positive anomalies.

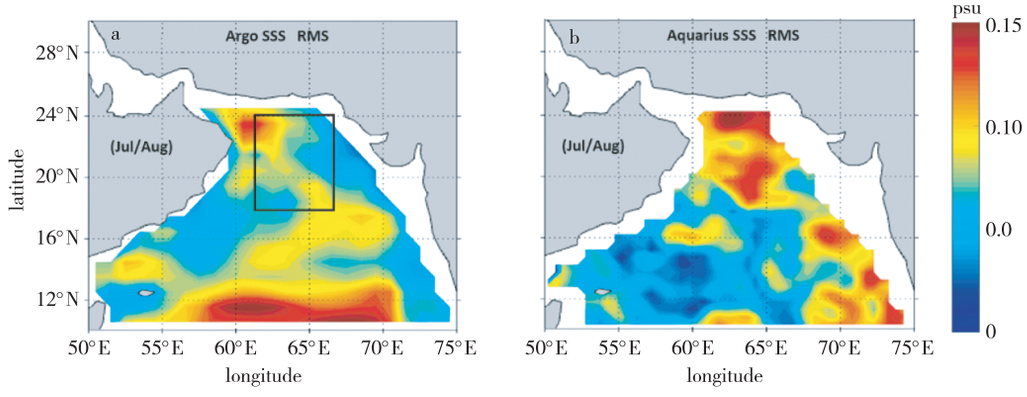

Fig. 6 RMS of SSS and time series of particular SSS data (multi-year averaged removed from each data sets) during July/August, (a) Argo SSS, and (b) Aquarius SSS

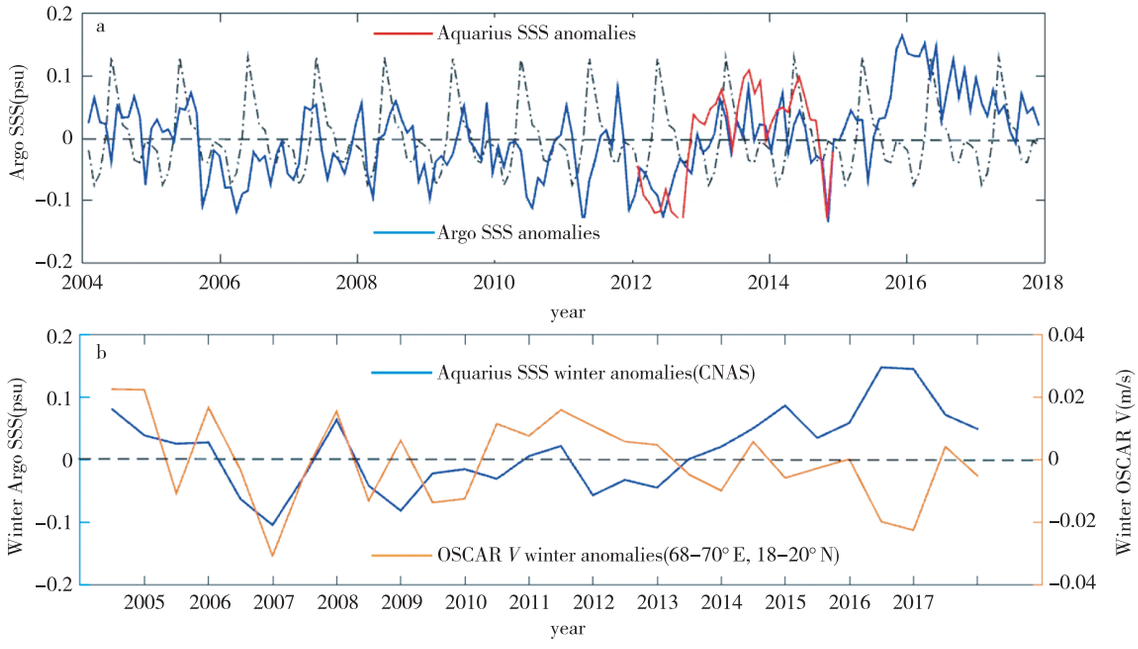

Fig. 7 (a)Time series of SSS anomalies of Argo (2004–2017) (blue curve) and Aquarius (2012–2014) (red curve) in the CNAS,here box averaged and remove the multiyear average;(b) Winter (DJF) anomalies for Argo SSS (blue curve) in CNAS,OSCAR *V* component (orange curve) for northeastern Arabian Sea (68–70°E,18–20°N)

Therefore the result can suggest that, when the northwestward advection reduces, it may cause SSS increase in the CNAS during winter. According to the strength of the northwestward flowing eastern Arabian coastal current, we can observe interannual variability in the CNAS. Exploring and studying this SSS observation is hoped to be useful for further researches and to make sustainable exploration and exploitation of ocean resources. Understanding the seasonal changes may help to improve the knowledge in weather conditions, and long term climate changes.

4 Summary and conclusion

In this study, satellite Aquarius, SMOS and in situ Argo observations were used to study the SSS variability in the CNAS. Although the mean state of SSS in CNAS is similar for all salinity data sources, SMOS was not used to study the SSS changes in inter-annual time scale due to its fabricated responses for external land induced contaminations. As a result of that, RMS of SMOS is giving less similarity, compared to the Aquarius and Argo observations. Both Argo and Aquarius show similar SSS variation on interannual time scale. Argo displays higher SSS measurements in CNAS compared with the other two satellites datasets.

CNAS records the highest SSS value of 36.7 psu which reduces to 36.3 psu southward in the CNAS. Due to the advection and excess evaporation, the CNAS SSS shows significant seasonal variation. As a result of southward advect, the high salinity water from the Gulf of Oman and the existence of Ras al Hadd Jet present the highest SSS anomalies during the mature phase of SW monsoon period in the CNAS. Coastal upwelling associated with summer monsoon favors the low salinity water intrusion to the studied area. The effect of the northwestward advection of low salinity West Indian coastal currents can be observed up to the Sea of Oman as negative SSS anomalies during later winter phase. The high salinity water of NAS advects to the most southeastern Arabian Sea during the later summer monsoon period. The strength of the monsoon circulation contributes to intensive inter-annual changes for SSS in the CNAS. It's necessary to do further studies to understand the subsurface salinity responses to the monsoon circulation and their associated climate changes in the central north Arabian Sea.

Acknowledgements: This study is supported by the National Natural Science Foundation of China (41525019, 41506019), the State Oceanic Administration of China (GASI-IPOVAI-02). The authors would like to thank the data providers that make this work possible. LOCEAN/IPSL provides SMOS salinity data (http://www.salinityremotesensing.ifremer.fr). NASA/GSFC/ODPS provides Aquarius SSS data (http://oceandata.sci.gsfc.nasa.gov). Argo gridded data is available in International Argo Program (http://www.argo.ucsd.edu). The OAFlux data is provided by WHOI OAFlux Project of Woods Hole Oceanographic Institution (http://oaflux.whoi.edu). Ocean surface currents data is available in OSCAR NOAA's Ocean Surface Current Analyses Real time (http://www.oscar.noaa.gov/index.html). GPCP precipitation data is available in the NASAGSFC (http://precip.gsfc.nasa.gov). Wind data from the ASCAT wind is available at IFREMER/CERSAT (http://cersat.ifremer.fr). Sea surface temperature data is OISST from NOAA/Earth System Research Laboratory (http://www.esrl.noaa.gov).

References

[1] Kumar P S, Narvekar J, Kumar A, et al. Intrusion of the Bay of Bengal water into the Arabian Sea during winter monsoon and associated chemical and biological response [J]. Geophys Res Lett, 2004, 31 (15), DOI: 10.1029/2004GL020247

[2] Shenoi S S C, Shankar D, Michael G S, et al. Hydrography and water masses in the southeastern Arabian Sea during March-June 2003 [J]. J Earth Syst Sci, 2005, 114(5): 475-491

[3] Schott F A, Xie S P, Mccreary J P. Indian Ocean circulation and climate variability [J]. Rev Geophys, 2009, 47(1), DOI: 10.1029/2007RG000245

[4] Shetye S R, Gouveia A D, Shenoi S S C. Circulation and water masses of the Arabian Sea [J]. P Indian As-Earth-Plan Sci, 1994, 103(2): 107-123

[5] Qasim S Z. Oceanography of the northern Arabian Sea [J]. Deep-Sea Res Pt I, 1982, 29(9): 1041-1068

[6] Kumar K G V, Kumar P K D, Smitha B R, et al. Hydrographic characterization of southeast Arabian Sea during the wane of southwest monsoon and spring intermonsoon [J]. Environ Monit Assess, 2008, 140(1/2/3): 231-247

[7] Rao R R, Sivakumar R. Seasonal variability of sea surface salinity and salt budget of the mixed layer of the north Indian Ocean [J]. J Geophys Res, 2003, 108(C1): 9-1-9-14

[8] Narvekar J, D'mello J R, Kumar S P, et al. Winter-time variability of the eastern Arabian Sea: a comparison between 2003 and 2013 [J]. Geophys Res Lett, 2017, 44(12): 6269-6277

[9] Shankar D, Vinayachandran P N, Unnikrishnan A S. The monsoon currents in the north Indian Ocean [J]. Prog Oceanogr, 2002, 52(1): 63-120

[10] Donguy J-D, Meyers G. Seasonal variation of sea: surface salinity and temperature in the tropical Indian Ocean [J]. Deep-Sea Res Pt I, 1996, 43(2): 117-138

[11] Gould W J, Roemmich D, Wijffels S, et al. Argo profiling floats bring new era of in situ ocean observations [J]. Eos Trans Amer Geophys Union, 2004, 85(19): 185-191

[12] Lagerloef G S E. Introduction to the special section: the role of surface salinity on upper ocean dynamics, air-sea interaction and climate [J]. J Geophys Res, 2002, 107(C12), DOI 10.1029/2002JC001669

[13] Chowdary J S, Gnanaseelan C, Thompson B, et al. Water mass properties and transports in the Arabian Sea from Argo observations [J]. J Atmos Ocean Sci, 2005, 10(3): 235-260

[14] Kumar S P, Prasad T P. Formation and spreading of Arabian Sea high-salinity water mass [J]. J Geophys Res, 1999, 104(C1): 1455-1464

[15] Zhang Y H, Du Y, Zheng S J, et al. Impact of Indian Ocean dipole on the salinity budget in the equatorial Indian Ocean [J]. J Geophys Res, 2013, 118(10): 4911-4923

[16] Du Y, Zhang Y H. Satellite and Argo observed surface salinity variations in the tropical Indian Ocean and their association with the Indian Ocean dipole mode [J]. J Climate, 2015, 28(2): 695-713

[17] Zhang Y H, Du Y. Seasonal variability of salinity budget and water exchange in the northern Indian Ocean from HYCOM assimilation [J]. Chin J Oceanol Limn, 2012, 30(6): 97-107

[18] Momin I M, Mitra A K, Prakash S, et al. Variability of sea surface salinity in the tropical Indian Ocean as inferred from Aquarius and in situ data sets [J]. Int J Remote Sens, 2015, 36(7): 1907-1920

[19] Momin I M, Mitra A K, Mahapatra D K, et al. Errata: review of recent evaluation of satellite estimates sea surface salinity in the tropical Indian Ocean [J]. J Appl Remote Sens, 2016, 10(4): 049901

[20] Moon J H, Song Y T. Seasonal salinity stratifications in the near-surface layer from Aquarius, Argo, and an ocean model: focusing on the tropical Atlantic/Indian Oceans [J]. J Geophys Res, 2014, 119(9): 6066-6077

[21] Bindlish R, Jackson T, Cosh M, et al. Global soil moisture from the Aquarius/SAC-D satellite: description and initial assessment [J]. IEEE Geosci Remote Sens Lett, 2015, 12(5): 923-927

[22] Adler R F, Huffman G, Chang A, et al. The version 2 Global Precipitation Climatology Project (GPCP) monthly precipitation analysis (1979—present) [J]. Hydrometeorol, 2003, 4(6): 1147-1167

[23] Yu L S, Jin X Z, Weller R. Multidecade global flux datasets from the Objectively Analyzed air-sea Fluxes (OAFlux) project: latent and sensible heat fluxes, ocean

evaporation,and related surface meteorological variables [R].Woods Hole Oceanographic Institution OAFlux Project Technical Report (OA-2008-01),2008

[24] Bentamy A,Fillon C D.Gridded surface wind fields from Metop/ASCAT measurements[J].Int J Remote Sens,2012,33(6):1729-1754

[25] Johnson E S,Bonjean F,Lagerloef G S,et al.Validation and error analysis of OSCAR sea surface currents[J].J Atmos Ocean Tech,2007,24(4):688-701

[26] Shankar D, Shetye S. On the dynamics of the Lakshadweep high and low in the southeastern Arabian Sea[J].J Geophys Res,1997,102 (C6):12551-12562

[27] Boutin J,Martin N,Reverdin G,et al.Sea surface freshening inferred from SMOS and ARGO salinity:impact of rain[J].Ocean Sci,2012,9(5):183-192

[28] Banks C J,Gommenginger C P,Srokosz M A,et al.Validating SMOS ocean surface salinity in the Atlantic with Argo and operational ocean model data[J].IEEE Trans Geosci Remote Sens,2012,50(5):1688-1702

[29] Drucker R,Riser S C.Validation ofaquarius sea surface salinity with Argo:analysis of error due to depth of measurement and vertical salinity stratification[J].J Geophys Res,2014,119(7):4626-4637

[30] Bohm E,Morrison J M,Manghnani V,et al.The Ras al Hadd Jet:remotely sensed and acoustic Doppler current profiler observations in 1994-1995[J].Deep-Sea Res Pt II,1999,46(8/9):1531-1549

[31] Joseph S,Freeland H J.Salinity variability in the Arabian Sea[J].Geophys Res Lett,2005,32(9):387-404

[32] Lee C M,Jones,B H,Brink K H,et al.The upper-ocean response to monsoonal forcing in the Arabian Sea:seasonal and spatial variability[J].Deep-Sea Res Pt II,2000,47(7/8):1177-1226

[33] Schott F A,Mccreary J J P.The monsoon circulation of the Indian Ocean[J].Prog Oceanogr,2001,51(1):1-123

[34] Morrison J M.Inter-monsoonal changes in the T-S properties of the near-surface waters of the Northern Arabian Sea[J].Geophys Res Lett,1997,24(21):2553-2556

[35] Wiggert J, Murtugudde R, Mcclain C. Processes controlling interannual variations in wintertime (northeast monsoon) primary productivity in the central Arabian Sea [J].Deep-Sea Res Pt II,2002,49(12):2319-2343

[36] Jensen T G.Arabian Sea and Bay of Bengal exchange of salt and tracers in an ocean model[J].Geophys Res Lett,2001,28(20):3967-3970

[37] Schneider T,Bischoff T,Haug G H.Migrations and dynamics of the intertropical convergence zone[J].Nature,2014,513(7516):45-53

[38] Schott F.Monsoon response of the Somali current and associated upwelling[J].J Geophys Res,1983,12(3):357-381

[39] Vinayachandran P N,Masumoto Y,Mikawa T,et al.Intrusion of the southwest monsoon current into the Bay of Bengal[J].J Geophys Res,1999,104(c5):11077-11085

[40] Boutin J,Martin N,Yin X B,et al.First assessment of SMOS data over open ocean.Part II:sea surface salinity [J].IEEE Trans Geosci Remote Sens,2012,50(5):662-1675